Nanoscale

COMMUNICATION

View Article Online
View Journal | View Issue

Cite this: *Nanoscale*, 2016, **8**, 5835

Received 29th December 2015,
Accepted 9th February 2016

DOI: 10.1039/c5nr09261b

www.rsc.org/nanoscale



# Exciton energy recycling from ZnO defect levels: towards electrically driven hybrid quantum-dot white light-emitting-diodes†

Xin Zhao,‡[a] Weizhen Liu,‡[a,b] Rui Chen,[a] Yuan Gao,[a] Binbin Zhu,[a] Hilmi Volkan Demir,[a,c,d] Shijie Wang[e] and Handong Sun*[a,f]

**An electrically driven quantum-dot hybrid white light-emitting diode is fabricated *via* spin coating CdSe quantum dots onto a GaN/ZnO nanorod matrix. For the first time, quantum dots are excited by fluorescence resonance energy transfer from the carriers trapped at surface defect levels. The prototype device exhibits achromatic emission, with a chromaticity coordinate of (0.327, 0.330), and correlated color temperature similar to sunlight.**

## 1. Introduction

Colloidal quantum dots (QDs) have provoked long-lasting research efforts towards low-cost, solution-processed next-generation solid-state lighting (SSL) in the past two decades.[1,2] Amongst potential applications of QDs in SSL, realizing white light-emitting-diodes (w-LEDs) has drawn tremendous attention.[3–6] On one hand, traditional lighting devices such as incandescent bulbs and compact fluorescence lights (CFLs) are power-inefficient.[7] According to a report by the energy information administration of the U.S., 412 billion kilowatt-hours (KWh) of electricity were consumed by lighting in 2014, taking up 11% of the gross electricity usage nationwide. With the development of smart phones and tablets, this ratio will no doubt keep increasing. Thus, w-LEDs which are environmentally friendly and more power-efficient are viewed as the most promising candidate to revolutionize the *status quo* in lighting. On the other hand, due to their outstanding merits of highly tunable luminescence and purity in color, QDs are considered as an ideal lumophore in w-LEDs.[8] Tuning of the band structure can be easily achieved by modulating the size or composition of the dots. In lieu of the high vacuum, elevated temperature and sophisticated equipment needed by the traditional semiconductor industry, QD synthesis is all solution-based reactions of accessible precursors, which is economically favorable.[9]

Aside from their feasibility in synthesis methods and versatile electronic band-structure, energy injection to these organic-ligand capped dots remains the main obstacle in the way towards practical electrically driven w-LED devices. To effectively excite quantum dots, several routes including exciting QDs by back-lit LEDs (PL mode) as well as injecting carriers *via* charge transport layers (EL mode) have been utilized.[10] As for the devices working in PL mode, the external quantum efficiency is largely restricted by the back-lit LED. Meanwhile for devices in the EL scheme, the limited conductivity of the organic charge transport layer and the carrier-injection polarity cause prototype devices to exhibit low EQE (~2%) and current densities.[8] Besides, the majority of these prototypes make use of only a single layer or a few layers of QDs as the lumophore, which are thought to be favorable for carrier injection and minimizing the interlayer energy transfer and quenching.[11] Yet the low loading ratios of QDs, on the other hand, severely limit the power output, impairing the development of high-luminance w-LEDs. Moreover, QD w-LEDs also require the mixing of several types of dots or physically combining multiple red, green and blue QD LEDs, preventing further device miniaturization. Thus, all-inorganic QD excitation schemes with high loading ratios as well as the ability for one-chip integration are highly desirable.

As another competitive building block of SSL, ZnO nanorods (NRs) have also attracted remarkable attention in the field of ultraviolet and blue optoelectronics.[12] The elevated exciton

[a]*Division of Physics and Applied Physics, School of Physical and Mathematical Sciences, Nanyang Technological University, 21 Nanyang Link, 637371, Singapore. E-mail: hdsun@ntu.edu.sg*
[b]*Centre for Advanced Optoelectronic Functional Materials Research and Key Laboratory of UV-Emitting Materials and Technology (Northeast Normal University), Ministry of Education, Changchun 130024, China*
[c]*School of Electrical and Electronic Engineering, Block S2.1, 50 Nanyang Avenue, Nanyang Technological University, 639798, Singapore*
[d]*Department of Electrical and Electronic Engineering, Department of Physics, UNAM-Institute of Materials Science and Nanotechnology, Bilkent University, Bilkent, Ankara, 06800, Turkey*
[e]*Institute of Materials Research and Engineering (IMRE), A*STAR (Agency for Science, Technology and Research), 2 Fusionopolis Way, Innovis, #08-03, 138634, Singapore*
[f]*Centre for Disruptive Photonic Technologies, School of Physical and Mathematical Sciences, Nanyang Technological University, SPMS-PAP-01-28, 21 Nanyang Link, 637371, Singapore*

†Electronic supplementary information (ESI) available. See DOI: 10.1039/c5nr09261b

‡These authors contributed equally to this work.

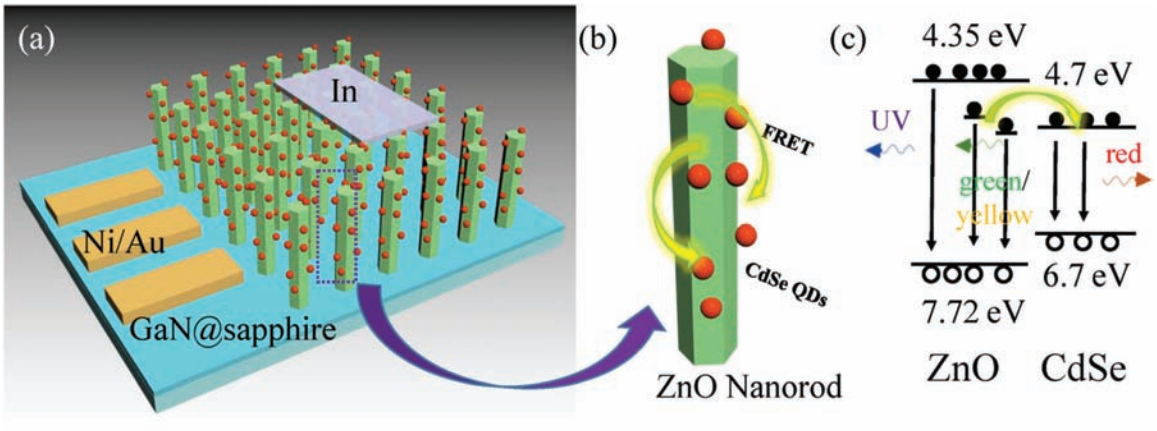


Fig. 1 (a) GaN/ZnO/CdSe quantum dot white light-emitting-diode schematic. (b) A magnified single QD-coated nanorod. (c) Band diagram depicting the idea of energy transfer from the DLE of ZnO NRs to CdSe. Both in (b) and (c), the yellow curved arrows refer to the energy transfer procedure from rods to quantum dots.



binding energy (~60 meV) together with the near defect-free nature of each rod makes them a key candidate for nano-photonics.[13,14] The miniaturization of the ZnO, on the other hand, results in a high surface-to-volume ratio, which would introduce a high density of defects as well as induced exciton-trapping, giving rise to visible (usually in green to yellow range) deep level emission (DLE) and other non-radiative recombination channels. Therefore, smart schemes to passivate the material–ambient interface and extract excitonic energy from the defects are key issues in realizing ZnO NR SSL devices.[15]

To extract the exciton energy from the surface defect sites and facilitate energy injection into QDs, we propose a novel lighting device design scheme as shown in Fig. 1 which integrates CdSe QDs onto a ZnO nanorod array surface. As has been demonstrated by 3D solar cells, ZnO nanowires are nearly defect-free single crystals which enlarge the mean free path of the carriers transporting in them. Thus, ZnO nanowire is an ideal charge transport layer (CTL) material system.[16] Aside from transporting carriers, the nanorod array acts as an excitation matrix for the QDs in this research. As shown in Fig. 1b the resonant energy transfer (FRET) from the nanorod defect level excites the CdSe as well as provides a competitive recombination route for captured excitons and carriers, reducing the excitonic energy loss in the DLE process. Moreover, the large surface area of ZnO nanorods enables a high packing density of QDs, which is favorable for high-brightness w-LED applications. Also, all of the RGB light sources are integrated in a 3D matrix on one-chip. Thus, the scheme is promising in realizing electrically injected QD w-LEDs which are highly integrable and a prototype device utilizing the scheme is demonstrated in the following passages.

## 2. Results and discussion

The ZnO sub-micro/nanorod (NR) array in this research was grown on commercially available p-type GaN@Sapphire substrate *via* a hydrothermal method. As shown in Fig. 2, the average circumscribed diameter of the NRs is around 800 nm and the length is about 4 μm. The height of the rods is highly uniform, which favors subsequent spin-coating and electrode deposition. The resultant rods display a hexagonal morphology indicating the growth direction along the *c*-axis and relatively high crystal quality.[17] The lack of peaks other than (002) and (004) shown in the ZnO X-ray diffraction pattern in Fig. 2c further confirms this argument.[18] To remove the surface contamination and to facilitate a demonstration of energy transfer to quantum dots, the rods are annealed in air atmosphere at 650 °C for 1 h. After annealing, pin holes appeared at the surface (in Fig. 2b and c), which were probably caused by the accumulation of oxygen vacancies and rearrangement of surface atoms.[15] The annealing procedure was introduced to suppress the near-band edge emission (NBE) and increase the

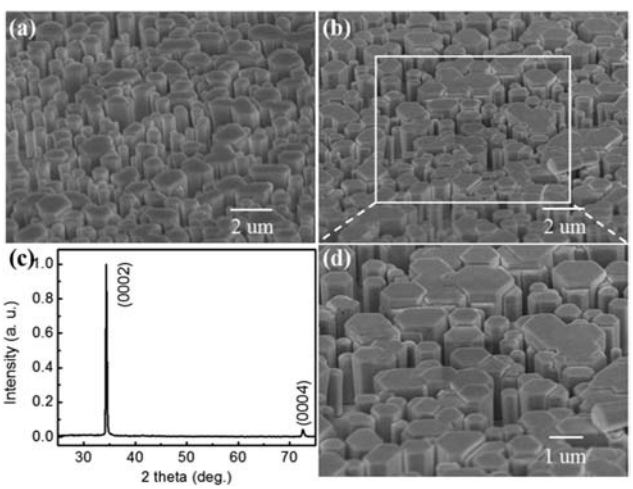


Fig. 2 (a) SEM image of the as-grown ZnO NR array on the GaN substrate. (b) ZnO NRs annealed in air for 1 h. (c) X-ray diffraction pattern of the rods in (b). (d) Magnification of (b) showing the small pin-holes at the rod surface.

density of deep level states for unambiguously observing the energy transfer procedure from DLE to the QDs as shown in the following optical measurements. Also, the removal of surface contamination (such as from HMT) was confirmed from the improved imaging quality due to less electron accumulation in the SEM characterization (Fig. S1†). Then, the CdSe QD solution is spin-coated onto the NRs. The transmission electron microscopy (TEM) images (Fig. S1c and S1d†) have shown that these QDs are highly uniform in size and the average diameter is around 5.0 nm. Fig. S1a and b† compare the top views of the annealed and spin-coated samples, though the size of the QDs is beyond the SEM resolution, it is still quite obvious that the infiltration of the QD solution replenished the gap between the rods and deteriorated the conductivity of the sample. Additionally, this assumption is supported by the *I–V* characterization (Fig. 5a).

The ZnO nanorods and CdSe QDs were characterized individually and as an assembly to investigate their optical properties by absorption and photoluminescence measurements. As shown in Fig. 3a, the PL of the ZnO nanorods consists of mainly two peaks, the near-band edge emission centered at 379 nm and a relatively strong deep-level emission covering the green to yellow region. The annealing quenches the NBE and strengthens the DLE by creating high density surface defects such as Zn and O vacancies.[19] The latter part of the spectrum overlaps well with the strong absorbing area of the CdSe QDs, which is critical for the energy transfer process. After integrating the QDs *via* spin-coating onto the ZnO nanorod array, a sharp peak emerged around the wavelength of 625 nm in Fig. 3b accompanied by the weakened green emission of ZnO. The red emission corresponds to the electron–hole pair recombination in CdSe QDs,[20] showing that the emission of QDs was not quenched after they were spin-coated onto the nanorod array. Considering the relative strength of the DLE compared to the pumping laser, the excitation of the QDs should be the direct absorption of the 325 nm excitation line of the He–Cd laser. However, the decrement in the DLE intensity implies that there may be energy transfer or a re-absorption effect induced by the QDs, which has been confirmed to exist in the following time-resolved PL measurement.[21]

To further confirm the feasibility of the FRET between the ZnO and QDs, we studied and compared the time-resolved PL (TRPL) spectra of the ZnO nanorods and that of the ZnO/QD assembly. The results are shown in Fig. 4 and the experimental details are listed in the Experimental section. Both of the transient PL spectra of the two samples show single exponential decay and the fitted lifetime of the ZnO green emission and the CdSe red emission are displayed in the legends in Fig. 4a and b. It is obvious that the lifetime of ZnO green emission is shortened and the lifetime of CdSe QDs is prolonged after them being integrated. Thus the energy transfer in the assembly has been confirmed. In this particular assembly, the ZnO acts as the donor and the attached quantum dots accept the transferred energy.[22]

From the formalism of FRET, the energy transfer efficiency can be extracted from the change in the lifetime of the donor, as shown in the following equation.[23]

$$\eta_{ET} = 1 - \frac{\tau}{\tau_0} = 17.07\%$$

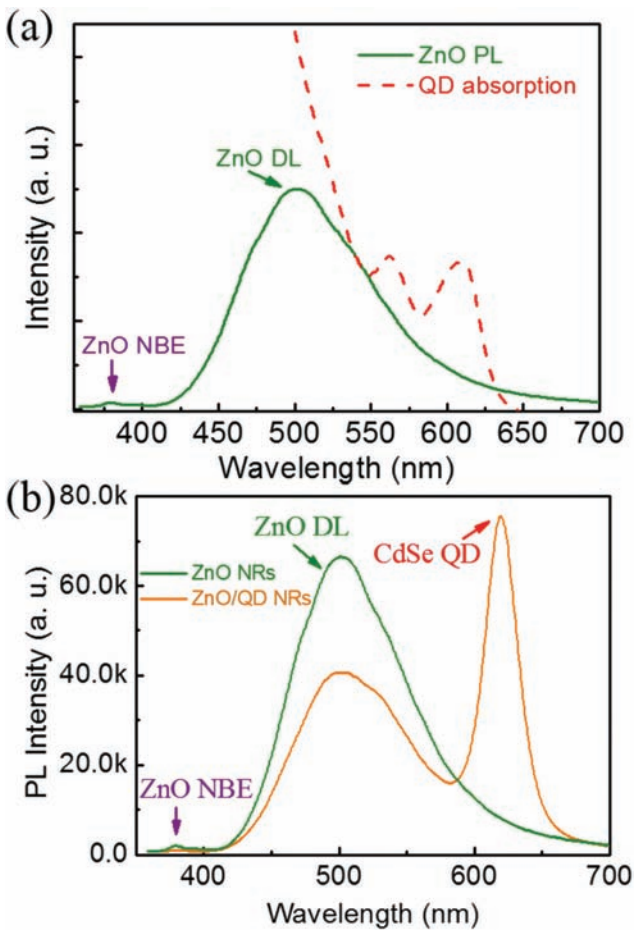


Fig. 3 (a) Photoluminescence spectrum of annealed ZnO and the absorption spectra of QDs in solution. (b) Photoluminescence of the ZnO nanorods and ZnO/QD assembly.

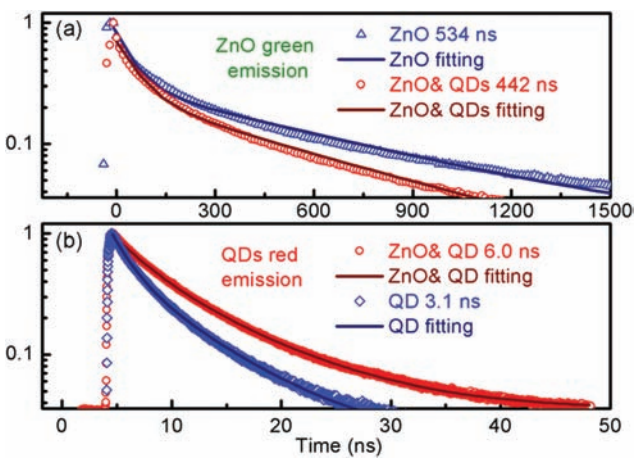


Fig. 4 Transient PL of (a) ZnO deep-level green emission and (b) CdSe red emission in the ZnO NRs and ZnO/QD assembly.

Herein, $\eta_{ET}$ refers to the FRET energy transfer efficiency. The symbols $\tau$ and $\tau_0$ refer to the lifetime of the donor luminescence with and without the presence of the acceptor. By substituting the lifetime with the experimental results, the energy transfer efficiency is calculated to be around 17%. Since the quantum dots that we utilized in this study have a relatively thick shell (~2.5 nm, accounting for the shell and surfactant),[24] the limiting factor of the energy transfer efficiency is suspected to be the distance between the ZnO matrix and the quantum dots. To support this speculation, the FRET efficiency can be calculated using the following equation,

$$\eta_{ET} = \frac{{R_0}^6}{r^6 + {R_0}^6}$$

$R_0$ and $r$ refer to the Foster distance and the donor–acceptor distance, respectively. Makhal *et al.*[25] have calculated the Foster distance in a ZnO-dye FRET system in which the system has a similar absorption–emission overlap. Thus it is reason-

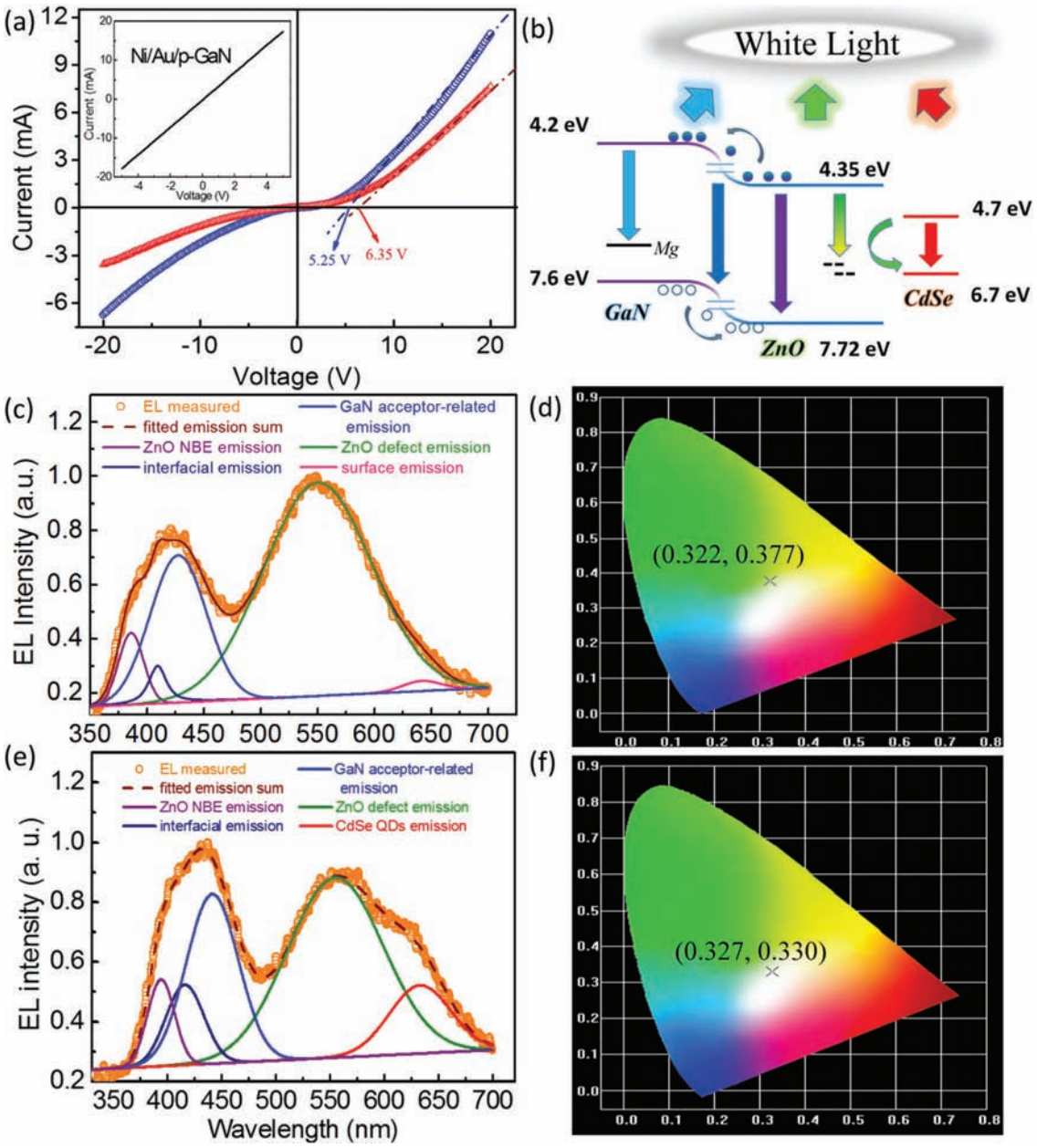


**Fig. 5** (a) *I–V* curve of the GaN/ZnO before and after the QD coating. The inset of (a) is the *I–V* curve of the Ni/Au contact on p-GaN. (b) Comprehensive Energy band diagram of GaN/ZnO/CdSe hybrid w-LED under forward bias. (c) EL spectrum of the GaN/ZnO heterostructure under forward bias without a QD coating. (d) CIE 1931 chromaticity coordinate of the device in (c). (e) EL spectrum of the GaN/ZnO/CdSe w-LED under forward bias. (f) CIE 1931 chromaticity coordinate of the device in (e).

 

able to estimate the $R_0$ to be 1.84 nm accordingly. By inserting the measured value of $\eta_{ET}$, the donor acceptor distance $r$ is calculated to be 2.4 nm, confirming the limiting factor of energy transfer to be the distance between the donor and acceptor. From another perspective, the matched distance further confirms the existence of energy transfer.

To examine the feasibility of fabricating a device based on the ZnO/QD system, a prototype device was fabricated directly using the above in-test GaN/ZnO/QD structure as shown in Fig. 1. Due to the highly uniform height of the ZnO nanorods, the cathode indium pad could be attached to the array using pressure. The anode Ni/Au electrode is fabricated on the GaN substrate through electron beam evaporation. As shown in the inset of Fig. 5a, the linear *I–V* curve proves that a good ohmic contact has formed, ruling out the possible Schottky contact induced rectification. The *I–V* curve of the device has shown a rectification behavior of the GaN/ZnO/QD LED as well as the GaN/ZnO matrix. The GaN/ZnO/QD device showed a turn-on phenomenon at around 6.35 V, which is reasonably close to the band gap of ZnO considering the potential drop at the ZnO/GaN interface as well as the two electrode contacts.[26] The relatively large reverse current is mainly caused by defects at the GaN/ZnO interface and nanorod surface.[27] These stress induced surface defects would act as a carrier source under reverse bias.[28] After the coating of the QDs, the leakage current is reduced due to the induced passivation of the nanorod surface as well as the insulating effect introduced by the QD thin film between the ZnO NR tips and indium electrodes.[29]

The electroluminescence (EL) of the GaN/ZnO heterostructure and GaN/ZnO/QD w-LED was measured using a home-made setup and the results are shown in Fig. 5c and e respectively. The EL spectra of the two devices were decomposed into multiple components originating from diverse recombination processes. These processes are elaborated in the energy band diagram of the GaN/ZnO/QD heterostructure w-LED shown in Fig. 5b. For the QD hybrid w-LED, the violet/blue region consists of mainly the NBE peak of ZnO (~380 nm), ZnO/GaN interfacial recombination which happened in the depletion region (~410 nm) and the transition between the p-type GaN conduction band electron to the Mg acceptor level.[30] The green component (~550 nm) and the red component (~625 nm) originate from the DLE of ZnO and electron–hole pair recombination in the QDs, respectively. The green curved arrow between the ZnO and CdSe QDs denotes the non-radiative energy transfer process. The RGB components constituted the overall observed white light emission. It is noteworthy to mention that, compared to that of the hybrid LED, the EL of the ZnO/GaN is lacking in red component and the weak peak in the orange-red region (640 nm) corresponds to a radiative transition between the two defect levels: $Zn_i$ and $O_i$.[31,32] The coated quantum dots quenched this recombination route due to the competitive consumption route for the captured electrons.

Complying with the Commission Internationale de L'Eclairage (CIE) 1931 standard, the chromaticity coordinates of the GaN/ZnO heterostructure itself displayed a CIE value of (0.322, 0.377), which fell in the olive region. After being integrated with the QDs, the CIE value turned out to be (0.327, 0.330), very close to the definition of an achromatic standard white light, which is (0.330, 0.330). The correlated color temperature (CCT) of the hybrid w-LED is calculated to be 5783 K, very close to the 5780 K color temperature of sunlight.[33] The natural feeling of white light emitted by the GaN/ZnO/QD hybrid LED shows promise for application in indoor lighting. Besides, the blue/green and green/red ratios can be tuned *via* changing the growth and annealing conditions of the nanorods.

It is necessary to mention that the energy injection into the QDs may happen in two parallel routes: one is the FRET energy transfer from the DLE that occurred near the surface to the QDs; the other is the absorption of the UV/blue light from the ZnO/GaN junction. So, it is interesting to justify which route is of more importance in our case. We suggested that the direct excitation from UV/blue EL contributed very limitedly to the luminescence of the QDs and the energy transfer contributed much more to the emission from the QDs. A schematic description of the EL propagation supporting this argument is shown in Fig. 6. According to Daniel Vanmaekelbergh *et al.*,[34] the NBE and DLE emissions originate from spatially isolated luminescence processes involving different recombination

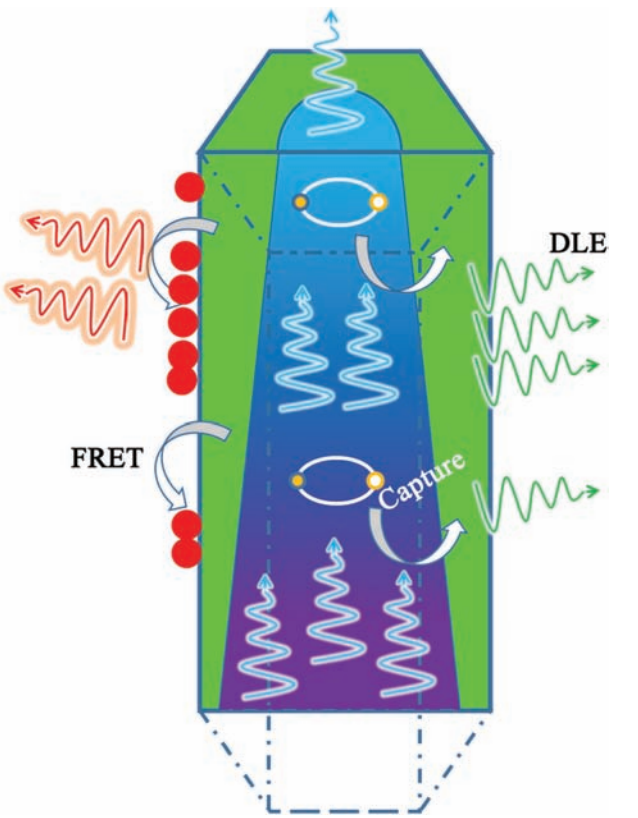


**Fig. 6** An evolutional schematic modelling of the electroluminescent light propagation in a single nanowire. The single wire is intersected in the $(10\bar{1}0)$ plane.

species. The NBE involves the recombination of excitons. Meanwhile, the DLE occurs near the surface throughout the rods. Due to the carrier injection polarity, the NBE mostly occurred at the ZnO/GaN interface, namely the p–n junction region. This deduction could be further justified by much stronger UV/blue emission in the EL spectra than in the PL spectra, in which the optical excitation and recombination mostly occurred near the upper tips of the nanorod array. Then, a portion of the EL emission light was wave-guided in an axial direction towards the top of the wire.[35]

Attributed to elevated oscillator strength of excitons in ZnO, the excitonic emission would interact strongly with the cavity excitons of the ZnO nanorods. As a result, excitons are generated throughout the wires. Yet, the defect sites are capable of capturing the generated excitons, especially when the NBE is transmitted in a radial direction towards the surface where the defect density is high. This phenomenon is demonstrated by the cone-like distribution of UV/blue light in the single wire, which takes into account both the radial and axial energy loss of NBE to DLE.

Thus, within the distance where effective FRET can occur (within 10 nm), the DLE is the dominating fluorescence process. On the other hand, in this study, we have employed QDs with thick ZnS shells (~2 nm) and small cores. ZnS possesses a larger band gap (3.54 eV, 300 K) than ZnO/GaN (3.3 eV, 300 K), which is not able to assist in harvesting the photons emitted by ZnO/GaN.[24] Thus in this device, the excitation of CdSe quantum dots originated from FRET.

## 3. Experimental section

### Fabrication of the ZnO nanorod array

ZnO nanorods are self-assembled on commercial p-GaN substrates *via* a hydrothermal route using 50 mmol $L^{-1}$ zinc acetate and HMT as the precursor (1 : 1). The precursor solution is heated and retained at 95 °C for 1 h in a convection oven. The resultant nanorod array is rinsed using deionized water followed by thermal annealing in air at 650 °C for 1 h to remove surface contamination.[17]

### Synthesis of CdSe/ZnS core–shell colloidal quantum dots

The synthesis of colloidal quantum dots was based on the published literature.[24] 128 mg of cadmium oxide (CdO, Sigma-Aldrich, 99.5%) and 367 mg of zinc acetate ($Zn(Ac)_2$, Sigma-Aldrich, 99.99%) were mixed with 5 mL of oleic acid (OA, Sigma-Aldrich, 90%) in a 50 mL three-neck flask. The mixture was degassed under vacuum at 120 °C for two hours. Then 25 mL of 1-octadecene (1-ODE, Sigma-Aldrich, 90%) was added into the reaction vessel. The temperature of the mixture was increased to 300 °C under an Ar atmosphere. 0.2 mmol of selenium (Se, Alfa Aesar, 99.999%) in 0.2 mL of trioctylphosphine (TOP, Sigma-Aldrich, 90%) was injected into the flask rapidly. After 2 min, 0.3 mL of dodecanethiol was injected into the mixture dropwise. The reaction was kept at 300 °C for 20 min, and then 2 mmol of sulfur (S, Sigma-Aldrich, 99.998%) in 1 mL of TOP was added. After 10 min, the reaction was terminated by reducing the temperature.

### Fabrication of GaN/ZnO/CdSe w-LED device

CdSe quantum dots were directly spin-coated on the annealed nanorod array. After the solvent dried, an indium platelet and Ni/Au electrode was fabricated as an n- and p-pad respectively. The indium electrode was formed using direct pressing whereas the Ni/Au electrode on p-GaN was formed using e-beam evaporation to get rid of the damage of the QDs at elevated temperature.

### Measurement and characterization

The morphology of the nanorods and the device were characterized using a field emission scanning electron microscope (Model JSM-6700F) and the QD diameter and morphology were measured using transmission electron microscopy (Model JEOL 2010f). The steady-state PL was measured using a home-built PL system. Samples were excited using a 325 nm line from a Hd–Cd continuous-wave laser and the fluorescence was dispersed by double gratings and collected using a Hamamatsu R928 photomultiplier tube. A lock-in amplifier was integrated in the system to increase the signal to noise ratio. Transient PL of the ZnO green emission was excited using a 325 nm laser line of a wavelength tunable pulsed laser (5 ns pulse width, repetition rate 20 Hz). The above mentioned PMT was applied to collect the green emission signal and the output was stored on a digital phosphor oscilloscope (Tektronix DPO 7254) and averaged over 500 periods to improve the signal-to-noise ratio. The QD lifetime was measured using DCS-120 Confocal Scanning FLIM Systems with a temporal resolution of 100 ps. The excitation wavelength was 375 nm.

## 4. Conclusions

In conclusion, a novel scheme to excite quantum dots by extracting energy from defect captured carriers of a ZnO nanorod matrix is shown in this research. The existence of FRET is confirmed *via* measuring the transient photoluminescence of the ZnO/CdSe assembly and energy transfer efficiency is calculated to be 17%. To demonstrate the effectiveness of this scheme, a w-LED is fabricated *via* a simple electrode deposition procedure and the EL spectra show that a color temperature very similar to sunlight has been achieved. This device works well in ambient air without a polymer spacer processing procedure. It is worthwhile to mention that both the blue/green ratio and the green/red ratio are straightforwardly tunable *via* various routes including changing the nanorod aspect ratio and growth conditions,[15] as well as changing the QD species. Integrating versatile QDs with the semiconductor nanorod family, as demonstrated in this research, paves the way to the next generation of high brightness lighting with tunable color and lower power consumption.

 

## Acknowledgements

X. Z and W. L. contributed equally to this work. This work was supported by the Competitive Research Program in National Research Foundation (NRF-CRP-6-2010-2) of Singapore, the Singapore Ministry of Education through the Academic Research Fund under Projects MOE 2011-T3-1-005 (Tier 3) and Tier 1-RG92/15, the Program of NSFC (No. 61505026) and the China Postdoctoral Science Foundation (No. 2015M580238).

## References

1 C. L. Salter, R. M. Stevenson, I. Farrer, C. A. Nicoll, D. A. Ritchie and A. J. Shields, *Nature*, 2010, **465**, 594–597.
2 J. M. Caruge, J. E. Halpert, V. Wood, V. Bulović and M. G. Bawendi, *Nat. Photonics*, 2008, **2**, 247–250.
3 D. I. Son, B. W. Kwon, D. H. Park, W. S. Seo, Y. Yi, B. Angadi, C. L. Lee and W. K. Choi, *Nat. Nanotechnol.*, 2012, **7**, 465–471.
4 M. A. Schreuder, K. Xiao, I. N. Ivanov, S. M. Weiss and S. J. Rosenthal, *Nano Lett.*, 2010, **10**, 573–576.
5 J. Song, J. Li, X. Li, L. Xu, Y. Dong and H. Zeng, *Adv. Mater.*, 2015, **27**, 7162–7167.
6 X. Li, Y. Liu, X. Song, H. Wang, H. Gu and H. Zeng, *Angew. Chem., Int. Ed.*, 2015, **54**, 1759–1764.
7 T. Pulli, T. Donsberg, T. Poikonen, F. Manoocheri, P. Karha and E. Ikonen, *Light: Sci. Appl.*, 2015, **4**, e332.
8 E. Jang, S. Jun, H. Jang, J. Lim, B. Kim and Y. Kim, *Adv. Mater.*, 2010, **22**, 3076–3080.
9 L. Qian, Y. Zheng, J. Xue and P. H. Holloway, *Nat. Photonics*, 2011, **5**, 543–548.
10 Y. Shirasaki, G. J. Supran, M. G. Bawendi and V. Bulović, *Nat. Photonics*, 2012, **7**, 13–23.
11 Q. Sun, Y. A. Wang, L. S. Li, D. Wang, T. Zhu, J. Xu, C. Yang and Y. Li, *Nat. Photonics*, 2007, **1**, 717–722.
12 X. Liu, L. Gu, Q. Zhang, J. Wu, Y. Long and Z. Fan, *Nat. Commun.*, 2014, **5**, 4007.
13 H. Ding, N. Pan, C. Ma, Y. Wu, J. Li, H. Cai, K. Zhang, G. Zhang, W. Ren, J. Li, Y. Luo, X. Wang and J. G. Hou, *Adv. Mater.*, 2014, **26**, 3035–3041.
14 C. Zhang, C. E. Marvinney, H. Y. Xu, W. Z. Liu, C. L. Wang, L. X. Zhang, J. N. Wang, J. G. Ma and Y. C. Liu, *Nanoscale*, 2015, **7**, 1073–1080.
15 X. Zhao, Y. Gao, Y. Wang, H. V. Demir, S. Wang and H. Sun, *Adv. Opt. Mater.*, 2015, **3**, 1066–1071.
16 Z. Fan, H. Razavi, J. W. Do, A. Moriwaki, O. Ergen, Y. L. Chueh, P. W. Leu, J. C. Ho, T. Takahashi, L. A. Reichertz, S. Neale, K. Yu, M. Wu, J. W. Ager and A. Javey, *Nat. Mater.*, 2009, **8**, 648–653.
17 W. Liu, Y. Liang, H. Xu, L. Wang, X. Zhang, Y. Liu and S. Hark, *J. Phys. Chem. C*, 2010, **114**, 16148–16152.
18 K. W. Liu, R. Chen, G. Z. Xing, T. Wu and H. D. Sun, *Appl. Phys. Lett.*, 2010, **96**, 023111.
19 V. Avrutin, M. A. Reshchikov, N. Izyumskaya, R. Shimada, S. W. Novak and H. Morkoç, *Mater. Res. Soc. Symp. Proc.*, 2009, **1109**, B06.
20 W. K. Bae, J. Kwak, J. Lim, D. Lee, M. K. Nam, K. Char, C. Lee and S. Lee, *Nano Lett.*, 2010, **10**, 2368–2373.
21 C. A. Leatherdale, W. K. Woo, F. V. Mikulec and M. G. Bawendi, *J. Phys. Chem. B*, 2002, **106**, 7619–7622.
22 K. F. Chou and A. M. Dennis, *Sensors*, 2015, **15**, 13288–13325.
23 K.-T. Kuo, D.-M. Liu, S.-Y. Chen and C.-C. Lin, *J. Mater. Chem.*, 2009, **19**, 6780.
24 W. K. Bae, J. Kwak, J. Lim, D. Lee, M. K. Nam, K. Char, C. Lee and S. Lee, *Nano Lett.*, 2010, **10**, 2368–2373.
25 A. Makhal, S. Sarkar, T. Bora, S. Baruah, J. Dutta, A. K. Raychaudhuri and S. K. Pal, *J. Phys. Chem. C*, 2010, **114**, 10390–10395.
26 J. Dai, Y. Ji, C. X. Xu, X. W. Sun, K. S. Leck and Z. G. Ju, *Appl. Phys. Lett.*, 2011, **99**, 063112.
27 D. C. Look, B. Claflin and H. E. Smith, *Appl. Phys. Lett.*, 2008, **92**, 122108.
28 S. M. Sze and K. K. Ng, *Physics of semiconductor devices*, Wiley, Hoboken, 3rd edn, 2007.
29 R. Chen, Y. Q. Shen, F. Xiao, B. Liu, G. G. Gurzadyan, Z. L. Dong, X. W. Sun and H. D. Sun, *J. Phys. Chem. C*, 2010, **114**, 18081–18084.
30 X. Ren, X. Zhang, N. Liu, L. Wen, L. Ding, Z. Ma, J. Su, L. Li, J. Han and Y. Gao, *Adv. Funct. Mater.*, 2015, **25**, 2182–2188.
31 S. Choi, B. C. Johnson, S. Castelletto, C. Ton-That, M. R. Phillips and I. Aharonovich, *Appl. Phys. Lett.*, 2014, **104**, 261101.
32 H. Zeng, G. Duan, Y. Li, S. Yang, X. Xu and W. Cai, *Adv. Funct. Mater.*, 2010, **20**, 561–572.
33 E. F. Schubert and J. K. Kim, *Science*, 2005, **308**, 1274–1278.
34 L. van Vugt, S. Rühle, P. Ravindran, H. Gerritsen, L. Kuipers and D. Vanmaekelbergh, *Phys. Rev. Lett.*, 2006, **97**, 147401.
35 W. Z. Liu, H. Y. Xu, C. L. Wang, L. X. Zhang, C. Zhang, S. Y. Sun, J. G. Ma, X. T. Zhang, J. N. Wang and Y. C. Liu, *Nanoscale*, 2013, **5**, 8634–8639.